Gas Processing Journal

Vol. 11, No. 1, 2023, pp. 73 - 82
http://gpj.ul.ac.ir

Research Paper

Determination of Tetrahydrofuran Hydrate Dissociation Conditions and Estimation of Kihara Potential Parameters

Maryam Raeisi[1], Jafar Javanmardi[1*], Seyyed Mohamad Jokar[1*], Ali Rasoolzadeh[2]

[1] Department of Petroleum and Gas Engineering, Shiraz University of Technology, Shiraz, Iran
[2] Department of Chemical Engineering, Faculty of Engineering, Behbahan Khatam Alanbia University of Technology, Behbahan, Iran.

Received: 2024-10-19 Revised: 2025-08-19 Accepted: 2025-09-15

Abstract: Tetrahydrofuran (THF) is widely utilized as a gas hydrate promoter. Therefore, an accurate calculation of the phase equilibria of systems containing THF + gas is of great interest. This article aims to apply the van der Waals-Platteeuw (vdW-P) solid solution model to compute the THF + gas hydrate equilibrium conditions. To optimize the Kihara potential parameters of THF, only half of the pure THF data, specifically data with THF mole fractions below 6%, were used. The Peng-Robinson equation of state (PR EoS) was employed to compute fugacities in the gas phase, while the UNIQUAC activity model was used for the calculation of the liquid phase activity. The phase equilibria for both pure THF and mixed hydrates (carbon dioxide + THF, methane + THF, nitrogen + THF) were calculated and compared with experimental data and the Strobel model using the old Kihara parameters across all THF concentration ranges. The average absolute errors of the presented model and the Strobel model for 190 experimental data points were 0.3 K and 0.4 K, respectively. The results demonstrated an acceptable level of agreement between experimental and anticipated data for the systems under investigation.

keywords: Tetrahydrofuran, Hydrate formation, vdW-P model, Kihara potential parameters.

1- Introduction

Gas hydrates, also known as clathrate hydrates, are crystalline compounds formed from water and other substances. Water (host) and small molecules (guest) interact to form these compounds under low temperatures and relatively high pressures. Hydrogen-bonded water creates cavities that enclose gas molecules such as CH_4, C_2H_6, and CO_2, as well as liquids like tetrahydrofuran (THF) [1]. Three common structures can form from gas hydrates: I (sI), II (sII), or H (sH) [1, 2]. Each structure contains several cage types. While sI and sII each have two cage types, Ripmeester et al. identified sH as being characterized by three unique cage types [3].

The most common challenge of gas hydrate formation within the gas industry is associated with the obstruction of oil and gas pipelines and related issues [4]. Recently, numerous studies have focused on the beneficial applications of hydrate formation in gas storage and separation, particularly for CO_2 and hydrogen fuel gas [5, 6]. The incorporation of certain organic compounds, known as thermodynamic hydrate promoters (THPs), represents an advancement in the potential application of hydrates. These organic compounds promote the formation of hydrates, whether they are soluble or insoluble in water. The promoting impact can be explained by either increasing the equilibrium temperature of hydrates at a given pressure or by decreasing the equilibrium pressure at a specific temperature [4,7[7]–[10].

The promotional impact of THF in the hydrate system has been well investigated. For gases like CO_2 and hydrogen, THF stabilizes sII hydrates, therefore facilitating more effective gas storage and transportation. Gas separation systems employ THF because it promotes selective hydrate formation. By lowering equilibrium pressures, it also promotes the development of technologies in hydrate-based refrigeration and desalination. THF is employed as a model

* **Corresponding Author.**
Authors' Email Address: M. Raeisi (maryam_tec@yahoo.com**), J. Javanmardi (**Javanmardi@sutech.ac.ir**), S. M. Jokar** (jokar@sutech.ac.ir**), A. Rasoolzadeh** (jokar@sutech.ac.ir)

http://dx.doi.org/10.22108/gpj.2025.142996.1140

chemical in research because it forms hydrates without requiring a help gas, which facilitates the creation and validation of thermodynamic models [1] . The introduction of aqueous THF solutions at concentrations below 6 mole% generally leads to a reduction in pressure during gas hydrate formation [11]. Several studies in the literature report the phase equilibrium measurements of methane + THF [8,9,11,12], CO_2 + THF [11,13–15], and nitrogen + THF [8,14] systems. Nevertheless, few studies have examined thermodynamic models for computing the dissociation conditions of pure or mixed-gas hydrates, including THF.

De Deugd et al. [9] utilized van der Waals-Platteeuw (vdW-P) solid solution theory to calculate the chemical potential of water in the hydrate phase. The model successfully computed the stability conditions of methane + THF hydrates. Seo et al. [8] developed a model that computed equilibrium conditions for methane + THF and nitrogen + THF. Lee et al. [16] developed an alternative model for hydrocarbon + hydrogen and hydrogen + THF hydrates. This model assumed that hydrate cavities could be occupied by multiple hydrogen molecules, which has been considered unrealistic [17–20]. Strobel et al. [21] successfully calculated the hydrogen + THF hydrate dissociation conditions. They presented a thermodynamic model on the basis of the CSMGem framework that accurately computed the phase behavior of various hydrates comprising THF and hydrogen. The model employed previously regressed Kihara potential values for all components except THF and H_2, and computed the formation conditions of hydrates containing THF. The mole percentage of THF in pure THF hydrate was below 20% and was used for parameter optimization. Mohammadi et al. [14] utilized artificial neural networks (ANNs) to determine the dissociation pressures of THF + CH_4, CO_2, or N_2 hydrates as a function of temperature and THF concentration. Pahlavanzadeh et al. [22] have reported the Langmuir constants for THF, 1,4-dioxane, and acetone. They successfully calculated the dissociation conditions of CH_4, N_2, and CO_2 in the presence of water-soluble THPs. The Peng-Robinson equation of state (PR EoS) and UNIFAC models were employed to calculate the fugacity of the gas phase and activity coefficients of water in the liquid phase, respectively. Herslund et al. [23] utilized experimental data for mixed hydrates of THF + CO_2 and THF + N_2 to determine the Kihara parameters of THF. Additionally, they presented new Kihara parameters for CO_2 and N_2. Utilizing these new parameters, they calculated the hydrate dissociation conditions of CO_2 + THF, N_2 + THF, and N_2 + CO_2 + THF.

This study employs 50% of the reported experimental data of pure THF at concentrations of below 6 mole% in aqueous solutions to optimize the Kihara potential parameters of THF. To validate the accuracy of the optimized parameters, dissociation conditions of hydrates for pure THF (with mole fraction lower than 20%), CO_2 + THF, CH_4 + THF, and N_2 + THF are anticipated and compared with the experimental data published in the literature. For this purpose, the model of vdW-P with the PR EoS has been coupled with the UNIQUAC activity model for the hydrate phase equilibrium calculations. Therefore, this work aims to obtain new Kihara potential parameters for THF using a novel procedure and to assess the accuracy of these parameters in various systems that include both pure THF and mixed hydrates.

This study exhibits the following novelties when compared to prior research:

1. Using the activity of water in the hydrate phase to optimize the Kihara potential parameter of THF.
2. Only 50% of the reported experimental data of pure THF at concentrations of below 6 mole% in aqueous solutions for the hydrate formation condition of pure THF are utilized to optimize the Kihara interaction parameters for THF.
3. In contrast to the work of Strobel et al. [21], the UNIQUAC activity model is employed rather than the Van Laar activity model.

2- Models and Methods

2-1 Thermodynamic Model

This article presents a model based on the vdW-P theory [24]. In a system where gas, hydrate, and aqueous phases coexist at equilibrium, the chemical potentials of water in the hydrate and aqueous phases are equal and can be expressed as follows:

$$\mu_w^H = \mu_w^L \tag{1}$$

Where μ indicates chemical potential, the subscript w refers to water, and the superscripts H and L refer to the hydrate and aqueous phases, respectively. The equality of these chemical potentials can be written as the equality of the chemical potential difference of water between the phases and the hypothetical empty hydrate phase, β :

$$\Delta\mu_w^{\beta-H} = \mu_w^\beta - \mu_w^H = \Delta\mu_w^{\beta-L} = \mu_w^\beta - \mu_w^L \tag{2}$$

The water chemical potential difference between phases H and β phases, is defined by [21, 24, 25,]:

$$\Delta\mu_w^{\beta-H} = RT\sum_m \upsilon_m \ln\left(1+\sum_j C_{mj} f_j\right) + RT\ln\gamma_w^H \tag{3}$$

where υ_m is the ratio of type m cavity to the number of water molecules in the unit hydrate cell, j runs over all guest components, C_{mj} is the Langmuir constant, f_j is the fugacity of component j, and γ is the activity coefficient. The fugacity of a component in a gas phase is obtained from the PR EoS [26]. Table1 presents the critical properties and acentric factors of components for the computation of fugacity.

Table 1. Critical properties and acentric factors of components [27]

Component	T_c (K)	P_c (MPa)	ω
Methane	190.56	4.599	0.0115
Nitrogen	126.20	3.399	0.0377
Carbon dioxide	304.21	7.383	0.2236
THF	540.15	5.190	0.2254

The THF fugacity in the liquid phase can be calculated by [4,9]:

$$f_{THF} = x_{THF}\,\gamma_{THF}\,P^{sat}_{THF}\,\phi^{sat}_{THF}\exp\left(\frac{v^{L}_{THF}\,(p-p^{sat}_{THF})}{RT}\right) \quad (4)$$

$$P^{sat}_{THF} = 10^{-6}\times\exp\left(54.898-\left(\frac{5305.4}{T}\right)-(4.7627\,\ln(T))+(1.4291\times10^{-17})\times T^{6}\right) \quad (5)$$

In Eq. (4), x_{THF} is the mole fraction of THF, P^{sat}_{THF} is the saturation pressure of THF at system temperature, which can be obtained in MPa using Eq. (5) [27], ϕ^{sat}_{THF} is the fugacity coefficient of pure liquid THF at system temperature and P^{sat}_{THF}, v^{L}_{THF} is the molar volume of pure liquid THF and has the value of 81.55 $cm^3.mol^{-1}$ [27], T stands for temperature, and γ_{THF} is the activity coefficient of THF. In this study, they are calculated using the UNIQUAC model [28] using the optimized parameters [29]. The following formula is utilized to determine CO_2 solubility in the aqueous liquid phase [30]:

$$x^{L}_{CO_2} = \frac{f^{G}_{CO_2}}{(u_1+u_2T)\exp\left(\left(u_3-(P\times10^{-3})^{u_4}\right)/(P\times10^{-3})^{u_4}\right)} \quad (6)$$

The superscript G represents the gas phase, and pressure, P, is in MPa. The solubility of CH_4 or N_2 in the liquid phase is ignored. Table 2 lists the values of parameters as well as the constants u_1-u_4, required in the Eq. (6).

Table 2. The parameters of Eq. (6) [30]

Parameter	Value
u_1 (MPa)	-725919.22
u_2 (MPa.K^{-1})	2898.54
u_3 (MPa)	0.05127
u_4 (No Unit)	-0.11228

The Langmuir constants are calculated from Eqs. (7) to (9) [25,31].

$$C_{mj} = \frac{4\pi}{KT}\int_0^{\infty}\exp\left(-\frac{\omega(r)}{KT}\right)r^2dr \quad (7)$$

$$\omega(r) = 2z\varepsilon\left[\frac{\sigma^{12}}{R^{11}r}\left(\delta^{10}+\frac{a}{R}\delta^{11}\right)-\frac{\sigma^{6}}{R^{5}r}\left(\delta^{4}+\frac{a}{R}\delta^{5}\right)\right] \quad (8)$$

$$\delta^{N} = \frac{1}{N}\left[\left(1-\frac{r}{R}-\frac{\alpha}{R}\right)^{-N}-\left(1+\frac{r}{R}-\frac{\alpha}{R}\right)^{-N}\right] \quad (9)$$

(N=4, 5, 10,11)

In the above equations, k is the Boltzmann constant, and $\omega(r)$ is the spherically symmetric cell potential, which is a function of the coordination number (z), cage radius (R), and Kihara potential parameters $(\alpha,\ \sigma,\ \text{and}\ \varepsilon)$. All required parameters, except the Kihara potential parameters of components, have been presented in Table 3.

Table 3. Geometric parameters of different hydrate structures [21, 25]

	Structure I		Structure II	
No. of water /unit cell	46		136	
Cavities/ unit cell	Small cavity	Large cavity	Small cavity	Large cavity
	2	6	16	8
Coordination number	20	24	20	28
Radius of cavity (Å)	3.95	4.33	3.91	4.73

The Kihara potential parameters of THF were optimized using the Shuffled Complex Evolution (SCE) algorithm and are exhibited in Table 4. This table also includes the Kihara potential parameters for methane, nitrogen, and CO_2.

Table 4. Kihara potential parameters of the guest molecules

Component	a (Å)	σ (Å)	ε/k (K)	Ref.
Methane	0.3834	3.14393	155.593	[1]
Nitrogen	0.3526	3.13512	127.426	[1]
CO_2	0.6805	2.97638	175.405	[1]
THF	0.9013	3.56214	291.568	This work

The water activity coefficient in the hydrate phase is computed by the following equations [21]:

$$\ln\gamma^{H}_{w} = \frac{\Delta g^{\beta}_{w_0}}{RT_0}+\frac{\Delta h^{\beta}_{w_0}}{R}\left(\frac{1}{T}-\frac{1}{T_0}\right)+\int_{P_0}^{P}\frac{\Delta\upsilon^{H}}{RT}dp \quad (10)$$

$$\Delta g^{\beta}_{w_0} = a\Delta\upsilon^{H} \quad (11)$$

$$\Delta h_{w_0}^{\beta} = b\Delta\upsilon^{H} \quad (12)$$

$$\upsilon^{\beta} = (\upsilon_0)^3 \exp\left[a_1(T-T_0)+a_2(T-T_0)^2+a_3(T-T_0)^3-K_H(P-P_0)\right] \quad (13)$$

The parameters required for Eqs. (11) to (13) are listed in Table 5.

Table 5. Parameters for Eqs. (11) to (13) [21]

structure	a (J.cm^{-3})	b (J.cm^{-3})	υ_0 (cm^3.mol^{-1})	a_1 (K^{-1})	a_2 (K^{-2})	a_3 (K^{-3})
I	25.74	-481.32	22.7712	3.3849×10^{-4}	5.4009×10^{-7}	-4.7694×10^{-11}
II	260.00	-68.64	22.9456	2.0297×10^{-4}	1.8511×10^{-7}	-1.8794×10^{-10}

K_H is given by Eq. (14):

$$K_H = \sum_{i=1}^{C} K_{iH}\theta_{iL} \quad (14)$$

Where the values of K_{iH} for THF are 1×10^{-12} (MPa^{-1}) and 1×10^{-11} (MPa^{-1}) for structures I and II, respectively.

$$\upsilon = \left(a_0 + \sum_m N_m \sum_i g(\theta_{im})\Delta r_{im}\right)^3 \quad (15)$$

Δv^H is the difference between Eqs. (13) and (15) [21]. The fractional occupancy (θ_{im}) can be obtained as follows:

$$\theta_{im} = \frac{C_{im} f_i}{1+\sum_j C_{im} f_i} \quad (16)$$

$$g(\theta_{im}) = \frac{(1+\eta_m)\theta_{im}}{1+\eta_m\theta_{im}} \exp\left[D_0 - \overline{D}\right] \quad (17)$$

(For small cavities)

$$g(\theta_{im}) = \frac{(1+\eta_m)\theta_{im}}{1+\eta_m\theta_{im}} \quad (18)$$

(For large cavities)

Where N_m is the number of type m cages in the hydrate, a_0 is the standard hydrate lattice parameter at T_0 and P_0, which is equal to 12.03 (Å) for structure I and 17.1 (Å) for structure II, and Δr_{im} is a repulsive constant for guest molecule i in type m cage. The empirically determined functions $g(\theta_{im})$ for small and large cavities of both structures are defined by Eqs. (17) and (18), respectively. η_m is the number of water molecules in the hydrate structure per coordination number of cage m, D_0 is the molecular diameter of the component from the reference structure (4.247 (Å) for sI, 5.745 (Å) for sII) [21], $\overline{D}$ is the average molecular diameter of the guest molecules in the hydrate, expressed as a fractional occupancy, and θ_{im} is the i component's fractional occupancy in type m cage. The THF molecular diameter and repulsive constants are provided in Table 6 [21].

Table 6. Molecular diameter and repulsive constants of THF [21]

Component	Diameter (Å)	Repulsive constants (Δr_{im}) (Å)			
		Small cavity sI	Large cavity sI	Small cavity sII	Large cavity s II
Tetrahydrofuran	5.726	0	2.9839×10^{-2}	0	3.1854×10^{-2}

In Eq. (2), the left term is defined by [32]:

$$\frac{\Delta\mu_W^{\beta-L}}{RT} = \frac{\Delta\mu_W^0}{RT} - \int_{T_0}^{T}\frac{\Delta h_W}{RT^2}dT + \int_0^P \frac{\Delta v_W}{RT}dP - RT\ln(\gamma_W \times x_W) \quad (19)$$

$$\Delta h_w = \Delta h_w^0 + \int_{T0}^{T} \Delta C_{PW}\, dT \quad (20)$$

Where the superscript 0 stands for the reference state and T_0 and P refer to the absolute temperature at the ice point and equilibrium pressure, respectively. The constants used in the Eqs. (19) and (20), are presented in Table 7.

Table 7. Thermodynamic reference properties of structures I and II [25]

Parameters	Structure I	Structure II
$\Delta\mu_W^0$ (J.mol^{-1})	1263.6	882.8
Δh_W^0 (J.mol^{-1})	-4858.9	-5202.2
Δv_w (Cm^3.mol^{-1})	4.6	5.0
ΔC_{p_w} (J.mol^{-1}.K^{-1})	-38.12+0.141 (T-273.15)	

3- Results and Discussion

Because THF has a promoting effect, it is expected that a rise in THF concentration in the liquid phase will either raise the hydrate equilibrium temperature at a specified pressure or lower the determined hydrate equilibrium pressure at a given temperature. The ideal amount of THF in water for a structure II hydrate, where the large cavity is filled with THF, is expected to be x_{THF} = 0.056 [11]. Beyond this concentration, the promoting impact begins to diminish. Optimization exclusively utilizes experimental data related to pure THF hydrate with THF concentrations under 6%.

Among the Kihara parameters, a (core radii) is determined from virial and viscosity relations [33], and the other two parameters (σ, ε), are optimized to fit calculations of the model. Only 50% of the experimental data of pure THF hydrate is used for optimization. All the experimental data have been collected from

isobaric systems [19, 13, 34–37], except the data set prepared by Makino et al. [38].

In contrast to the compounds investigated in this work, THF hydrate forms from a liquid mixture of water and THF. Therefore, the last term of Eq. (3) should be considered for optimization of THF Kihara parameters and calculation of dissociation conditions of pure THF hydrate. The optimized THF Kihara parameters were previously presented in Table 4.

To examine the modeling accuracy, the optimized parameters were used to calculate the conditions of hydrate formation in pure THF, CO_2 + THF, CH_4 + THF, and N_2 + THF systems. The modeling findings and the experimental data from various references were compared in Figures 1-4.

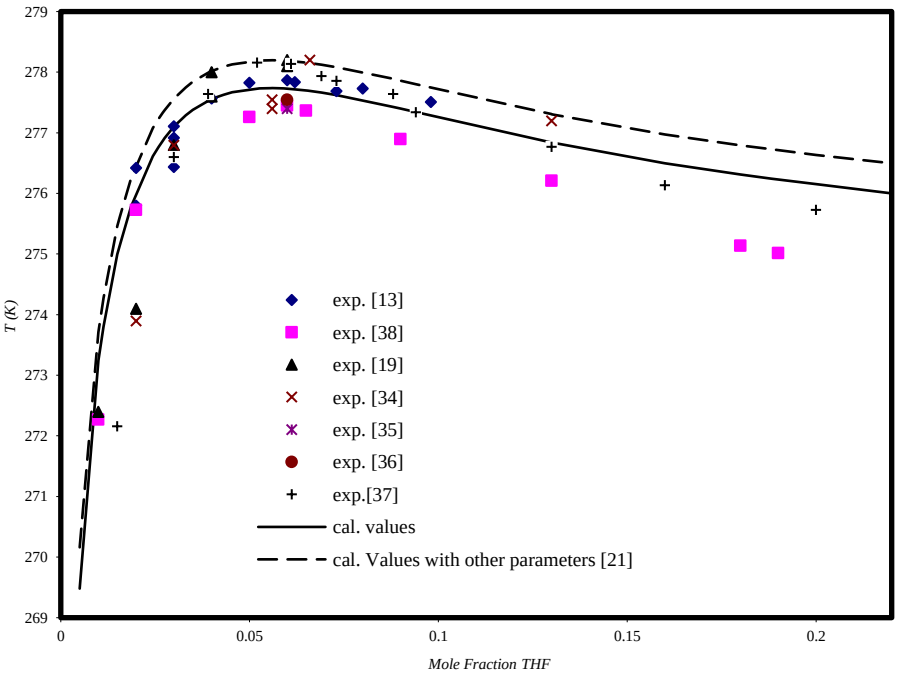

Fig 1. The expected and experimental conditions for pure THF hydrate dissociation at 1 bar. (Symbols reflect the experimental data, the solid lines represent the modeling results using the optimized Kihara parameters, and the dashed lines represent the modeling results with the Kihara parameters obtained from reference [21].)

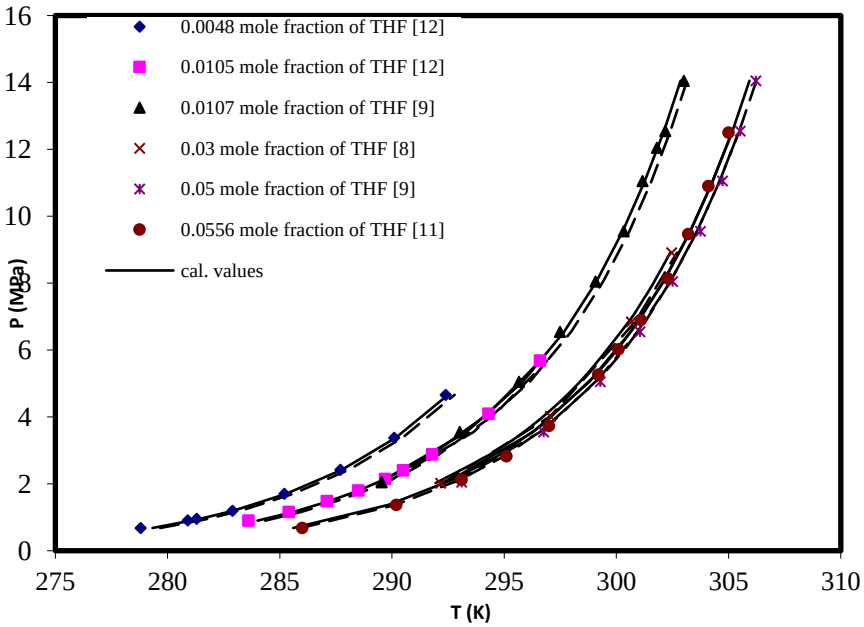

Fig 2. CH_4 + THF hydrate dissociation conditions (Symbols reflect the experimental data, the solid lines represent the modeling results using the optimized Kihara parameters, and the dashed lines represent the modeling results with the Kihara parameters obtained from reference [21].)

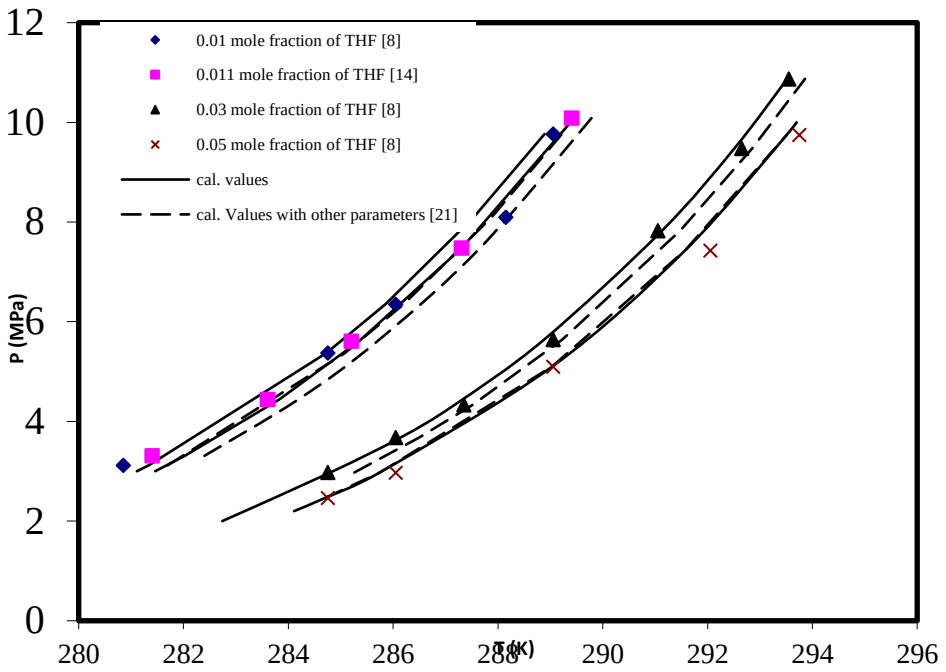

Fig 3. Conditions for the dissociation of N_2 + THF hydrate (Symbols reflect the experimental data, the solid lines represent the modeling results using the optimized Kihara parameters, and the dashed lines represent the modeling results with the Kihara parameters obtained from reference [21].)

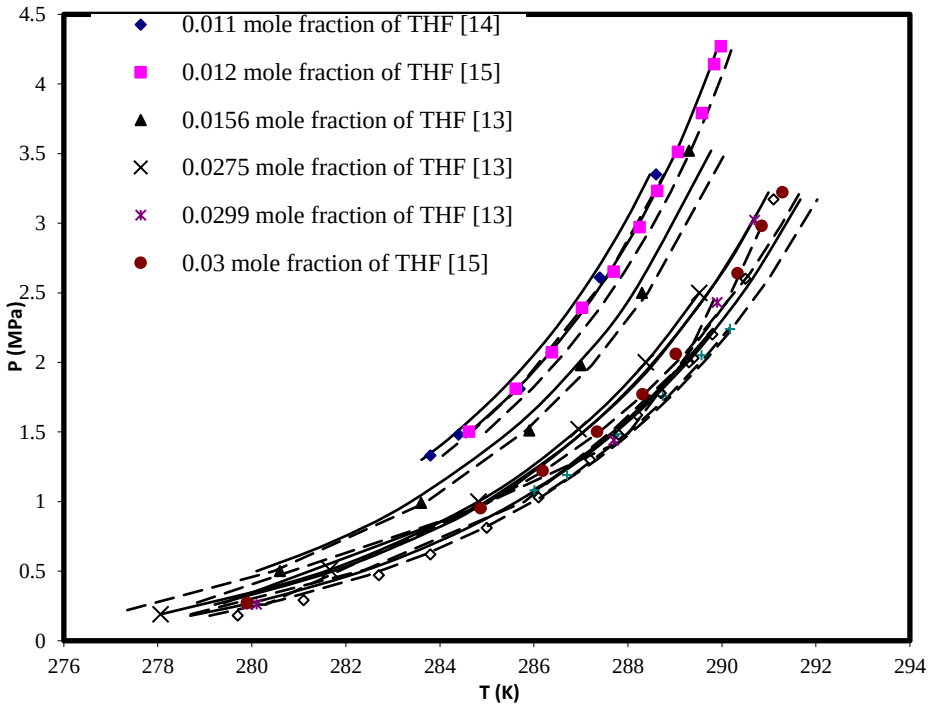

Fig 4. Conditions for the experimental and anticipated dissociation of CO_2 + THF hydrate (Symbols reflect the experimental data, the solid lines represent the modeling results using the optimized Kihara parameters, and the dashed lines represent the modeling results with the Kihara parameters obtained from reference [21].)

For pure THF, despite utilizing just 50% of the experimental data for modeling, a satisfactory agreement is observed between the experimental data and model calculations across the whole concentration range (Figure 1). The thermodynamic package with the newly optimized Kihara parameters yielded more accurate results for the mixed hydrates

(CH_4 + THF, N_2 + THF, and CO_2 + THF) compared to model calculations performed using the older version of the Kihara parameters. Table 8 is a report detailing the average absolute errors (AAE) associated with pure THF hydrate dissociation conditions calculations.

According to Table 8, the AAE of the thermodynamic package was reduced by more than 30 percent by the utilization of the newly optimized Kihara parameters. This indicates that optimized Kihara parameters can markedly enhance the precision of gas hydrate equilibrium calculations. The corresponding AAE for hydrate systems of CH_4 + THF, N_2 + THF, and CO_2 + THF are given in Tables 9-11. As can be shown, reasonable agreement is also obtained between the experimental results and the calculated ones for these systems. The results below indicate that the optimized Kihara parameters not only give accurate results for pure THF hydrate but also for the mixed gas hydrates.

Table 8. Average absolute error (AAE*) of temperature calculated with currently optimized Kihara parameters for pure THF hydrate

Mole fraction of THF range	No. of data points	Strobel et al. [21] (AAE* (K))	This work (AAE* (K))	Ref.
0.01-0.2	34	0.63	0.42	[19,13,34–38]
0.01-0.06	21	0.67	0.43	

$$^{*}AAE = \frac{1}{NP}\sum_{i=1}^{NP}\left|T_{cal} - T_{\exp}\right|$$

Table 9. AAE of temperature calculated with currently optimized Kihara parameters for CH_4 + THF mixed hydrate

Mole fraction of THF in aqueous solution	No. of data points	Pressure range, (MPa)	Strobel et al. [21] (AAE (K))	This work (AAE (K))	Data Ref.
0.0048	8	0.68-4.66	0.48	0.16	[12]
0.0105	9	0.90-5.68	0.40	0.08	[12]
0.0107	9	2.05-14.05	0.36	0.12	[9]
0.0300	4	2.02-8.91	0.13	0.18	[8]
0.0500	9	2.05-14.05	0.14	0.43	[9]
0.0556	12	0.68-12.50	0.20	0.22	[11]
overall	**51**		**0.29**	**0.20**	

Table 10. AAE of temperature calculated with currently optimized Kihara parameters for N_2 + THF mixed hydrate

Mole fraction of THF in aqueous solution	No. of data points	Pressure range, (MPa)	Strobel et al. [19] (AAE (K))	This work (AAE (K))	Data Ref.
0.0100	5	3.12-9.77	0.35	0.30	[8]
0.0110	5	3.31-10.09	0.57	0.22	[14]
0.0300	7	2.98-10.87	0.32	0.11	[8]
0.0500	5	2.20-10.00	0.56	0.22	[8]
overall	**22**		**0.42**	**0.22**	

Table 11. AAE of temperature calculated with currently optimized Kihara parameters for CO_2 + THF mixed hydrate

Mole fraction of THF in aqueous solution	No. of data points	Pressure range, (MPa)	Strobel et al. [19] (AAE (K))	This work (AAE (K))	Data Ref.
0.0110	5	1.30-3.35	0.17	0.17	[14]
0.0120	11	1.50-4.30	0.27	0.06	[15]
0.0156	6	0.50-3.52	0.24	0.32	[13]
0.0275	6	0.19-2.50	0.47	0.72	[13]
0.0299	4	0.26-3.02	0.29	0.49	[13]
0.0300	9	0.27-3.20	0.13	0.30	[15]
0.0500	6	1.08-2.24	0.16	0.20	[15]
0.0556	15	0.18-3.17	0.32	0.33	[11]
overall	**62**		**0.27**	**0.29**	

It was observed that it is not possible for the existing model to anticipate the data of Delahaye et al. [13] for dissociation conditions of carbon dioxide hydrate precisely (Table 11). Certain data points with lower concentrations correspond to temperatures that are either higher or equal to those with higher concentrations [21]. Therefore, it seems that the deficiency of the model in this case is related to the low accuracy of the reported experimental data. Finally, with the comparison of the results of Tables 8 to 11, it was interpreted that the optimized Kihara parameters give consistent results for sII pure THF hydrates and sII mixed hydrates. This indicates that one set of parameters may

accurately describe both pure and mixed hydrate equilibrium conditions. This consistency among systems is necessary for accurate modeling of hydrate equilibrium conditions in practical cases, including gas storage and transport applications. The presented model with the optimized Kihara parameters was also evaluated against the experimental data that was not used in the optimization process. The model stayed very accurate in these external tests, which shows that it is strong and can be used in many different situations, which is important for predictive modeling.

4- Conclusions

In this work, the Kihara potential parameters of THF in the hydrate phase were optimized. The vdW-P solid solution theory was applied to compute the dissociation conditions of pure THF hydrate and hydrates of CH4, N2, and CO2 with THF as a water-soluble hydrate promoter. Although only a few experimental data of pure THF hydrate formation conditions were used in the optimization procedure, the obtained results indicated high accuracy of the optimized Kihara potential parameters. Furthermore, it was concluded that, unlike the van Laar activity model, the UNIQUAC activity model could estimate the phase equilibrium condition of pure THF hydrate at higher concentrations up to 0.06 THF mole fraction. The overall temperature average absolute error for 190 valid experimental data points was about 0.30 K, showing this fact. As a conclusion, the current model had the most calculation power compared to those reported in the literature.

Acknowledgements

The Shiraz University of Technology assisted in this work, for which the authors are thankful.

References

[1] E.D. Sloan Jr, C.A. Koh, Clathrate hydrates of natural gases, CRC Press. (2007).

[2] D.W. Davidson, Clathrate hydrates, in: Water a comprehensive treatise, V. 2: Water in crystalline hydrates, aqueous solutions of simple nonelectrolytes, Springer. (1973).

[3] J.A. Ripmeester, J.S. Tse, C.I. Ratcliffe, B.M. Powell, A new clathrate hydrate structure, Nature. 325 (1987). https://doi.org/10.1038/325135a0.

[4] M.D. Jager, R.M. De Deugd, C.J. Peters, J. de Swaan Arons, E.D. Sloan, Experimental determination and modeling of structure II hydrates in mixtures of methane + water + 1, 4-dioxane, Fluid Phase Equilibria. 165 (1999) 209-23. https://doi.org/10.1016/S0378-3812(99)00278-2.

[5] S. Changyu, L. Wenzhi, Y. Xin, L.I. Fengguang, Y.U. Qing, M.U. Liang, C.H. Jun, L.I. Bei, C.H. Guangjin, Progress in research of gas hydrate, Chinese Journal of Chemical Engineering. 19 (2011) 151-62. https://doi.org/10.1016/S1004-9541(09)60192-0.

[6] A. Eslamimanesh, A.H. Mohammadi, D. Richon, P. Naidoo, D. Ramjugernath, Application of gas hydrate formation in separation processes: A review of experimental studies, The Journal of Chemical Thermodynamics. 46 (2012) 62-71. https://doi.org/10.1016/j.jct.2011.10.006.

[7] S. Mainusch, C.J. Peters, J. de Swaan Arons, J. Javanmardi, M. Moshfeghian, Experimental determination and modeling of methane hydrates in mixtures of acetone and water, Journal of Chemical & Engineering Data. 42 (1997) 948-50. https://doi.org/10.1021/je970039s.

[8] Y.T. Seo, S.P. Kang, H. Lee, Experimental determination and thermodynamic modeling of methane and nitrogen hydrates in the presence of THF, propylene oxide, 1, 4-dioxane and acetone, Fluid Phase Equilibria. 189 (2001) 99-110. https://doi.org/10.1016/S0378-3812(01)00580-5.

[9] R.M. De Deugd, M.D. Jager, J. de Swaan Arons, Mixed hydrates of methane and water-soluble hydrocarbons modeling of empirical results, AIChE Journal. 47 (2001) 693-704. https://doi.org/10.1002/aic.690470316.

[10] Y. Saito, Methane storage in hydrate phase with water soluble guests, InProc., 2nd Intnl Conf. on Natural Gas Hydrates (1996) 459-465.

[11] Y.J. Lee, T. Kawamura, Y. Yamamoto, J.H. Yoon, Phase Equilibrium Studies of Tetrahydrofuran (THF) + CH_4, THF + CO_2, CH_4 + CO_2, and THF + CO_2 + CH_4 Hydrates, Journal of Chemical & Engineering Data. 57 (2012) 3543-8. https://doi.org/10.1021/je300850q.

[12] A.H. Mohammadi, D. Richon, Phase equilibria of clathrate hydrates of tetrahydrofuran+ hydrogen sulfide and tetrahydrofuran + methane, Industrial & Engineering Chemistry Research. 48 (2009) 7838-41. https://doi.org/10.1021/ie900774v.

[13] A. Delahaye, L. Fournaison, S. Marinhas, I. Chatti, J.P. Petitet, D. Dalmazzone, W. Fürst, Effect of THF on equilibrium pressure and dissociation enthalpy of CO_2 hydrates applied to secondary refrigeration, Industrial & Engineering Chemistry Research. 45 (2006) 391-7. https://doi.org/10.1021/ie050356p.

[14] A.H. Mohammadi, J.F. Martínez-López,

D. Richon, Determining phase diagrams of tetrahydrofuran + methane, carbon dioxide or nitrogen clathrate hydrates using an artificial neural network algorithm, Chemical Engineering Science. 65 (2010) 6059-63. https://doi.org/10.1016/j.ces.2010.07.013.

[15] K.M. Sabil, C.J. Peters, Phase equilibrium data of mixed carbon dioxide and tetrahydrofuran clathrate hydrate in aqueous electrolyte solutions, in: 2007 AIChE Annual Meeting. (2007).

[16] S. Lee, P. Yedlapalli, J.W. Lee, Excess Gibbs potential model for multicomponent hydrogen clathrates, The Journal of Physical Chemistry B. 110 (2006) 26122-8. https://doi.org/10.1021/jp063431y.

[17] T.A. Strobel, C.J. Taylor, K.C. Hester, S.F. Dec, C.A. Koh, K.T. Miller, E.D. Sloan, Molecular hydrogen storage in binary THF– H_2 clathrate hydrates, The Journal of Physical Chemistry B. 110 (2006) 17121-5. https://doi.org/10.1021/jp062139n.

[18] K.C. Hester, T.A. Strobel, E.D. Sloan, C.A. Koh, A. Huq, A.J. Schultz, Molecular hydrogen occupancy in binary THF–H_2 clathrate hydrates by high resolution neutron diffraction, The Journal of Physical Chemistry B. 110 (2006) 14024-7. https://doi.org/10.1021/jp063164w.

[19] R. Anderson, A. Chapoy, B. Tohidi, Phase relations and binary clathrate hydrate formation in the system H_2– THF– H_2O, Langmuir. 23 (2007) 3440-4. https://doi.org/10.1021/la063189m.

[20] F.M. Mulder, M. Wagemaker, L. Van Eijck, G.J. Kearley, Hydrogen in porous tetrahydrofuran clathrate hydrate, ChemPhysChem. 9 (2008) 1331-7. https://doi.org/10.1002/cphc.200700833.

[21] T.A. Strobel, C.A. Koh, E.D. Sloan, Thermodynamic predictions of various tetrahydrofuran and hydrogen clathrate hydrates, Fluid Phase Equilibria. 280 (2009) 61-7. https://doi.org/10.1016/j.fluid.2009.02.012.

[22] H. Pahlavanzadeh, A. Kamran-Pirzaman, A.H. Mohammadi, Thermodynamic modeling of pressure–temperature phase diagrams of binary clathrate hydrates of methane, carbon dioxide or nitrogen+ tetrahydrofuran, 1, 4-dioxane or acetone, Fluid Phase Equilibria. 320 (2012) 32-7. https://doi.org/10.1016/j.fluid.2012.01.010.

[23] P.J. Herslund, K. Thomsen, J. Abildskov, N. von Solms, Modelling of tetrahydrofuran promoted gas hydrate systems for carbon dioxide capture processes, Fluid Phase Equilibria. 375 (2014) 45-65. https://doi.org/10.1016/j.fluid.2014.04.031.

[24] J.H. van der Waals, J.C. Platteeuw, Clathrate solutions, in: Advances in chemical physics, 2. (1959) 1-57. https://doi.org/10.1002/9780470143483.ch1.

[25] W.R. Parrish, J.M. Prausnitz, Dissociation pressures of gas hydrates formed by gas mixtures, Industrial & Engineering Chemistry Process Design and Development. 11 (1972) 26-35. https://doi.org/10.1021/i260041a006.

[26] D.Y. Peng, D.B. Robinson, A new two-constant equation of state. Industrial & Engineering Chemistry Fundamentals. 15 (1976) 59-64. https://doi.org/10.1021/i160057a011.

[27] M. Doble, Perry's chemical engineers' handbook, McGraw-Hill: New York, NY, USA. (1984).

[28] J.M. Prausnitz, R.N. Lichtenthaler, E.G. De Azevedo, Molecular thermodynamics of fluid-phase equilibria, Pearson Education. (1998).

[29] M. Sabil, K. Bin, Phase behaviour, thermodynamics and kinetics of clathrate hydrate systems of carbon dioxide in presence of tetrahydrofuran and electrolytes, Doctoral Thesis. (2009). https://resolver.tudelft.nl/uuid:07985423-55bb-45d2-82a9-7c24be4a0f34.

[30] J. Javanmardi, M. Moshfeghian, R.N. Maddox, Simple method for predicting gas-hydrate-forming conditions in aqueous mixed-electrolyte solutions, Energy & Fuels. 12 (1998) 219-22. https://doi.org/10.1021/ef9701652.

[31] V. McKoy, O. Sinanoğlu, Theory of dissociation pressures of some gas hydrates, The Journal of Chemical Physics. 38 (1963) 2946-56. https://doi.org/10.1063/1.1733625.

[32] G.D. Holder, G. Corbin, K.D. Papadopoulos, Thermodynamic and molecular properties of gas hydrates from mixtures containing methane, argon, and krypton, Industrial & Engineering Chemistry Fundamentals. 19 (1980) 282-6. https://doi.org/10.1021/i160075a008.

[33] L.S. Tee, S. Gotoh, W.E. Stewart, Molecular parameters for normal fluids. Kihara potential with spherical core, Industrial & Engineering Chemistry Fundamentals. 5 (1966) 363-7. https://doi.org/10.1021/i160019a012.

[34] H.J. Hanley, G.J. Meyers, J.W. White, E.D. Sloan, The melting curve of tetrahydrofuran hydrate in D_2O, International Journal of Thermophysics. 10 (1989) 903-9. https://doi.org/10.1007/BF00514485.

[35] D.G. Leaist, J.J. Murray, M.L. Post, D.W. Davidson, Enthalpies of decomposition and heat capacities of ethylene oxide and tetrahydrofuran

hydrates, The Journal of Physical Chemistry. 86 (1982) 4175-8. https://doi.org/10.1021/j100218a017.

[36] S.R. Gough, D.W. Davidson, Composition of tetrahydrofuran hydrate and the effect of pressure on the decomposition, Canadian Journal of Chemistry. 49 (1971) 2691-9. https://doi.org/10.1139/v71-447.

[37] Y.A. Dyadin, E.G. Larionov, A.Y. Manakov, F.V. Zhurko, E.Y. Aladko, T.V. Mikina, V.Y. Komarov, Clathrate hydrates of hydrogen and neon, Mendeleev Communications. 9 (1999) 209-10. https://doi.org/10.1070/MC1999v009n05ABEH001104.

[38] T. Makino, T. Sugahara, K. Ohgaki, Stability boundaries of tetrahydrofuran + water system. Journal of Chemical & Engineering Data. 50 (2005) 2058-60. https://doi.org/10.1021/je0502694.